

Application of Nonlinear Currents Approach in Analyzing Nonlinearly Loaded Dipole Antennas under Multi-tone Excitations

Bahareh Ja'fari Mohaddeseh Salehi
BSC student from BSC student from
Arak University Arak University

Saeed Reza Ostadzadeh¹
Assistant professor from Arak
University

Abstract

In this paper, the validity of nonlinear currents approach in analyzing nonlinear dipoles under multi-tone excitations is investigated. It is carried out via comparison with harmonic balance technique. The simulation results show that for single and infinite array of nonlinear dipoles with incident wave magnitude less than 0.1V/m, an acceptable error less than 5% and 11% is achieved respectively. In two cases, for incident waves of higher-valued amplitude, the nonlinear current approach results in violated response. Although there is a restriction on the use of nonlinear currents approach for the problem under consideration, comparison of the run-time of this approach with harmonic balance (HB) show that it is very efficient.

Keywords: Nonlinear currents approach; harmonic balance, nonlinear dipole.

Introduction

As known, nonlinear antennas in single and array arrangements can be used to control scattering response [1-14] (as frequency selective surface (FSS)) or to protect receivers against high-valued signals such as lightning strokes [15, 16]. There are several attempts either in frequency domain [1-14] or time domain [15, 16]. Among these approaches, Kun-Chu Lee et al proposed a number of frequency-domain approaches, for instance, nonlinear currents approach [9], genetic algorithm (GA) [6], neural networks based on radial basis functions (RBF) [10, 11] and so on. In [9], based on nonlinear currents approach (NC), closed-form solutions for harmonics scattered from nonlinear dipoles were extracted, and its validity in nonlinearly loaded antenna and antenna array under single-tone was investigated, but its validity of this approach in analyzing such structures under multi-tone excitations was not addressed. In addition, the computational efficiency of this approach in comparison with accurate models was not investigated. Hence in this study, validity and efficiency of the nonlinear currents approach in analyzing nonlinear dipoles under multi-tone excitations is carried.

This paper is organized as follows. In section II, the problem formulation based on nonlinear currents approach is briefly explained. Section III is focused on applying the approach on nonlinear dipoles under multi-tone excitation and validity range is extracted. Finally concluding remarks are given in section IV.

Nonlinear Current Approach

In this section, the modeling approach namely nonlinear currents approach is briefly explained. Figure 1 shows a dipole antenna centrally loaded by a p-n junction diode. With reference to [9], the analysis is based on the nonlinear equivalent circuit as shown in figure 2. Similarly, infinite array of nonlinear dipoles, as well as its equivalent circuit, are shown in figure 3 and 4 respectively. In figure 2 and 4, Y_{in} and I_{sc} denote Norton's equivalent circuit viewed across dipole terminal. These two quantities are computed via applying numerical methods such as the method of moments (MoM) [17] on Maxwell's equations. In dealing with nonlinearly loaded antennas based on nonlinear current approach, the nonlinear load is first represented as power series, i.e.

$$i = g_1 v + g_2 v^2 + g_3 v^3 + \dots$$

(1)

The voltage in (1) can be expressed as

$$v(t) = v^1(t) + v^2(t) + v^3(t) + \dots$$

(2)

Where $v^{(k)}(t)$ represents the sum of all mixing frequency components of k th order. If the voltage across the nonlinear load is limited to third order, the current $i(t)$ in (2) can be divided into linear term $i_{linear}(t)$ and nonlinear term $i_{nonlinear}(t)$ as bellow

$$i_{linear}(t) = g_1 v(t)$$

(3)

$$i_{nonlinear}(t) = g_2 v^2(t) + g_3 v^3(t)$$

(4)

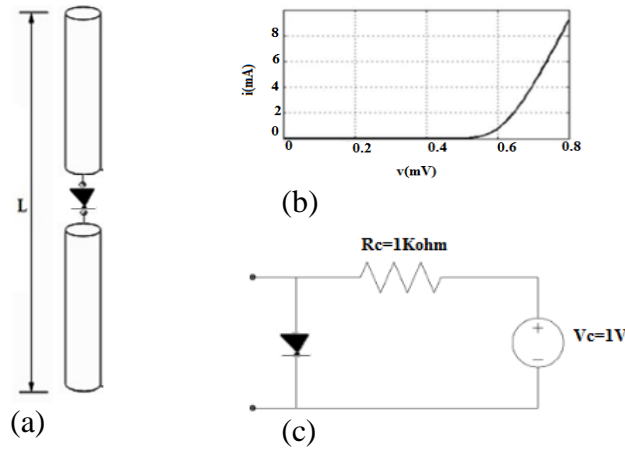


Figure (1) Schematic diagram of (a): single dipole loaded with p-n junction diode at its center, and (b): (i-v)

characteristic of the biased diode, (c): DC-biased circuit of the diode

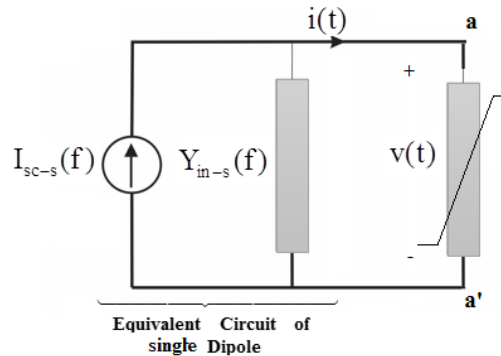


Figure (2) Nonlinear equivalent circuit of single nonlinear dipole.

The linear part in (1) represents a linear resistor with resistance of $1/g_1$. If the nonlinearity of the load is limited to third-degree then the mixing frequency components of third order are as bellow

$$i_{\text{nonlinear}}(t) = \{g_1 v^{(1)}(t)^2\} + \{2g_2[v^{(1)}(t)][v^{(2)}(t)] + g_3[v^{(1)}(t)]^3\} \quad (5)$$

The above equation can be divided into the second-order mixing component $i^{(2)}(t)$, and third-order mixing component $i^{(3)}(t)$, i.e.

$$i_{\text{nonlinear}}(t) = i^{(2)}(t) + i^{(3)}(t) \quad (6)$$

Where

$$i^{(2)}(t) = g_2[v^{(1)}(t)]^2 \quad (7)$$

and

$$i^{(3)}(t) = 2g_2[v^{(1)}(t)][v^{(2)}(t)] + g_3[v^{(1)}(t)]^3 \quad (8)$$

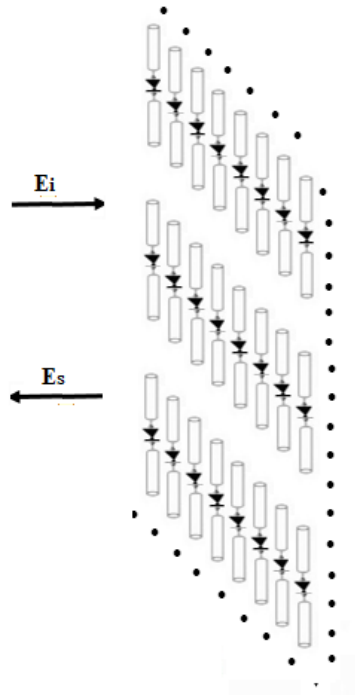


Figure (3) Schematic diagram of infinite array of dipoles centrally loaded with p-n junction diode.

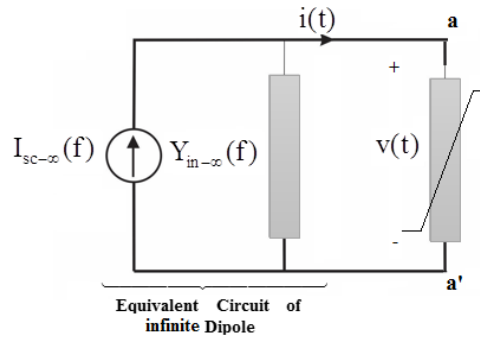


Figure (4) Nonlinear equivalent circuit of infinite array of nonlinear dipoles.

According to (7) and (8), the nonlinear equivalent circuit in figures 2 and 4 can be redrawn as shown in figure 5.

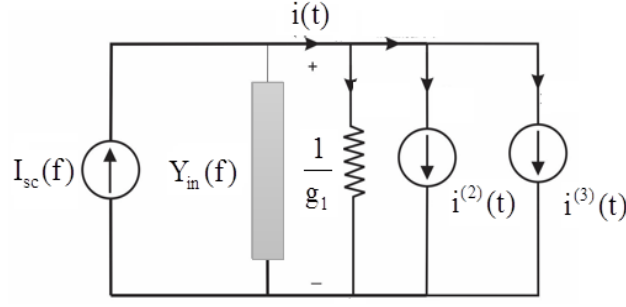


Figure (5) Representation of figures 2 and 4 based on nonlinear currents approach.

The goal of analysis is to obtain the terminal voltage of each dipole. Using the substitution theorem and setting all the current sources except $i_{sc}(t)$ to be zero initially, i.e., $i^{(2)}(t) = 0$ and $i^{(3)}(t) = 0$, one can obtain the voltage component from the contribution of $i_{sc}(t)$ only. This voltage component is regarded as $v^{(1)}(t)$ in (7) and (8). The total iteration sequence is given as

$$\left. \begin{array}{l} v^{(1)} \\ \text{linear} \end{array} \right| \begin{array}{l} \rightarrow i^{(2)}(t) \rightarrow v^{(2)}(t) \rightarrow i^{(3)}(t) \rightarrow v^{(3)}(t) \\ \leftarrow \text{nonlinear part (method of nonlinear currents)} \end{array}$$

(9)

For instance, assume that we have a multi-tone excitation

$$i_s(t) = \sum_{q=-Q}^{+Q} I_q^s e^{j\omega_q t}$$

(10)

By setting all the current sources except $i_{sc}(t)$ to be zero initially, one can obtain

$$v^{(1)}(t) = \sum_{q=-Q}^{+Q} V_q^{(1)} e^{j\omega_q t}$$

(11)

Where $V_q^{(1)} = I_q^s / (Y_{in}(\omega_q) + g_1)$. From (7) the current source $i^{(2)}(t)$ becomes

$$i^{(2)}(t) = g_2 \sum_{q_1=-Q}^{+Q} \sum_{q_2=-Q}^{+Q} V_{q_1}^{(1)} V_{q_2}^{(2)} e^{j(\omega_{q_1} + \omega_{q_2})t}$$

(12)

Similarly by setting all current sources except $i^{(2)}(t)$ to be zero, one can obtain

$$v^{(2)}(t) = \sum_{q_1=-Q}^{+Q} \sum_{q_2=-Q}^{+Q} \frac{g_2 V_{q_1}^{(1)} V_{q_2}^{(2)}}{Y_{in}(\omega_{q_1} + \omega_{q_2}) + g_1} e^{j(\omega_{q_1} + \omega_{q_2})t}$$

(13)

From (8)

$$i^{(3)}(t) = 2g_2 \sum_{q_1=-Q}^{+Q} \sum_{q_2=-Q}^{+Q} \sum_{q_3=-Q}^{+Q} \frac{-g_2 V_{q_1}^{(1)} V_{q_2}^{(1)} V_{q_3}^{(1)}}{Y_{in}(\omega_{q_2} + \omega_{q_3}) + g_1} \times e^{j(\omega_{q_1} + \omega_{q_2} + \omega_{q_3})t}$$

$$+ g_3 \sum_{q_1=-Q}^{+Q} \sum_{q_2=-Q}^{+Q} \sum_{q_3=-Q}^{+Q} V_{q_1}^{(1)} V_{q_2}^{(1)} V_{q_3}^{(1)} \times e^{j(\omega_{q_1} + \omega_{q_2} + \omega_{q_3})t}$$

(14)

and the third-order voltage caused by $i^{(3)}(t)$

is then given in (15)

$$v^{(3)}(t) = 2g_2 \sum_{q_1=-Q}^{+Q} \sum_{q_2=-Q}^{+Q} \sum_{q_3=-Q}^{+Q} \frac{g_2 V_{q_1}^{(1)} V_{q_2}^{(2)} V_{q_3}^{(3)}}{Y_{in}(\omega_{q_1} + \omega_{q_2} + \omega_{q_3}) + g_1} \times \frac{e^{j(\omega_{q_1} + \omega_{q_2} + \omega_{q_3})t}}{Y_{in}(\omega_{q_1} + \omega_{q_2} + \omega_{q_3}) + g_1} - g_3 \sum_{q_1=-Q}^{+Q} \sum_{q_2=-Q}^{+Q} \sum_{q_3=-Q}^{+Q} \frac{V_{q_1}^{(1)} V_{q_2}^{(2)} V_{q_3}^{(3)}}{Y_{in}(\omega_{q_1} + \omega_{q_2} + \omega_{q_3}) + g_1} \times e^{j(\omega_{q_1} + \omega_{q_2} + \omega_{q_3})t}$$

(15)

The total voltage response $v(t)$ can be found from (2), (11), (13), and (15). The scattering or radiating characteristics of the antenna can then be determined accordingly. Further information about this modeling approach in more detail can be found in [9].

Nonlinear Analysis under Multi-tone Excitation

Now in this section, the modeling approach in the previous section is applied on the single nonlinear dipole and infinite array of nonlinear dipoles. Each dipole is 1m long and has the length to diameter ratio of 74.2.

The nonlinear dipole is illuminated normally

by an incident plane wave containing two frequencies 140MHz and 160MHz. The nonlinear load is a biased p-n junction diode as shown in figure 1(b). Such a nonlinear load can be used in FSS applications [4]. In figure 1(b), the $i-v$ characteristic of the diode is expressed as bellow

$$i = I_s (e^{v/v_T} - 1)$$

(16)

Where $I_s = 10\text{nA}$, $v_T = 26\text{mV}$. Under the assumption of third-order nonlinearity for the biased diode, the coefficients for power series are listed in Table 1. Now applying the proposed approach on single and infinite array of nonlinear dipoles, under different wave magnitudes and finally comparison with HB, the acceptable range for nonlinear current approach is extracted.

Table 1-Series Fourier coefficient for the biased diode.

$i = I_s (e^{v/v_T} - 1) \approx g_0 + g_1 v + g_2 v^2 + g_3 v^3$			
$g_0(\text{A})$	$g_1(\text{A/V})$	$g_2(\text{A/V}^2)$	$g_3(\text{A/V}^3)$
0.00	0.027	0.52	6.6
7			

The magnitude of incident plane wave illuminating normally the nonlinear antenna is $E_i = 1\text{V/m}$. If the nonlinearity of the diode is limited to 3, then 12 mixing frequency components for the induced voltage across diode are generated. For this value of magnitude, the induced voltage across the diode is shown in figure 7. As seen, the simulation results by HB are in good agreement with figure 6 in [1]. In addition, the similar results by NC are shown in the same figure which is in disagreement with HB.

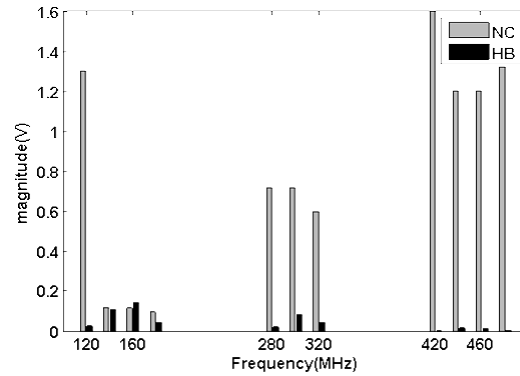


Figure (7) Spectral content across the diode for $E_i = 1\text{V/m}$.

Hence, to know the acceptable value for E_i , the same problem is tested for a few values of E_i as shown in figure 8. The simulation results show that when E_i increases, disagreement between the two approaches is increased. Figure 9 shows that for $E_i < 0.1\text{V/m}$ the maximum of relative error between the two approaches at each harmony is approximately less than 5% which is acceptable in electromagnetic engineering

point of view. Above this value for E_i , this approach results in unacceptable results. To know how mutual coupling effects influence the extracted value for E_i , similar simulations can be carried out for infinite array of nonlinear dipoles. The simulation results show that for such an array, the allowable value for E_i is once more 0.1V/m , but the relative error percentage is about 11% as shown in figure 9. Of course such a value is also acceptable.

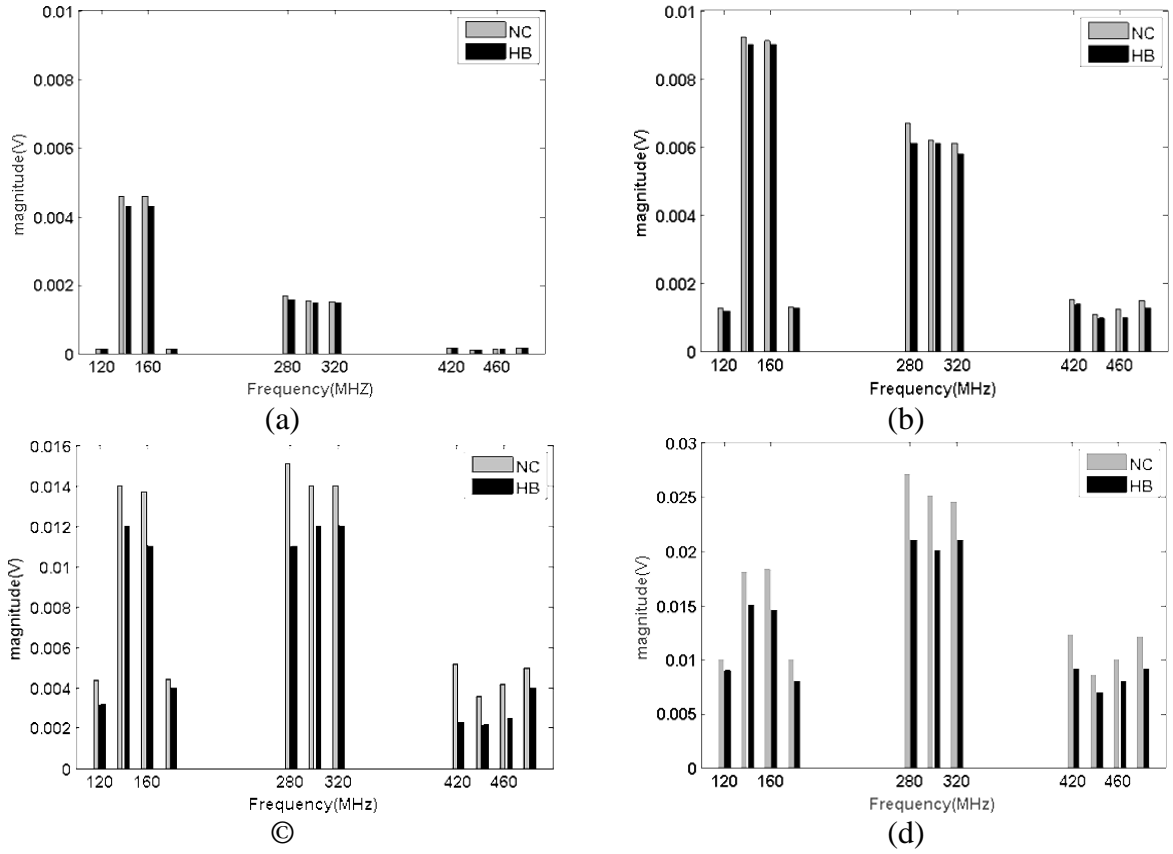


Figure (8) Spectral content across the diode for (a): $E_i = 0.05 \text{ V/m}$, (b): $E_i = 0.1 \text{ V/m}$, (c): $E_i = 0.15 \text{ V/m}$, and (d): $E_i = 0.2 \text{ V/m}$.

It is worth mentioning that although the nonlinear current approach is restricted to low-valued signals, according the

formulation in section II, it is computationally efficient.

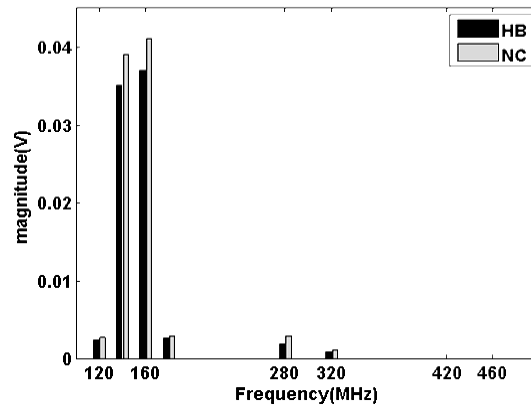


Figure (9) Spectral content across the diode in infinite array of nonlinear dipole for $E_i = 0.1 \text{ V/m}$.

Conclusion

In this study, the NC-based modeling approach was used to extract its validity interval in analyzing nonlinear dipoles both in single and in array arrangements. To this end, all NC-based computations were

compared with HB technique, and the following key findings were achieved:

1-In single and infinite array of nonlinear dipoles, for an incident wave with magnitude greater than 0.1 V/m , violated results is achieved.

2-The mutual coupling among nonlinear dipoles decreases the validity of the NC in the problem under consideration.

3-The validity range mentioned above was extracted for a strongly nonlinear load. Evidently, this range is extended for more weakly nonlinear loads and oblique incidences.

4-The computation time by NC is considerably less than the accurate models.

The above conditions make the nonlinear currents approach suitable in practical applications of nonlinear dipoles such as microwave imaging [18, 19], Frequency selective surfaces (FSS) [4].

References

- [1] C.C. Huang and T.H. Chu, "Analysis of wire scatterers with nonlinear or time-harmonic loads in the frequency domain," *IEEE Trans. Antennas Propagat*, vol. 41, pp. 25–30, 1993.
- [2] T.K. Sarkar and D.D. Weiner, "Scattering analysis of nonlinearly loaded dipole antennas," *IEEE Trans. Antenna Propag*, vol. 24, pp. 125–131, 1976.
- [3] T.K. Sarkar and D.D. Weiner, "Analysis of nonlinearly loaded multiport antenna structures over an imperfect ground plane using the Volterra-series method," *IEEE Trans. Electromag Compat*, vol. 20, pp. 278–287, 1978.
- [4] V. Fusco et al, "Microwave Phase Conjugation Using nonlinearly Loaded Wire Arrays," *IEEE Trans. Antennas Propagat*, vol. 54, no. 1, pp. 192–203, Jan. 2006.
- [5] K.C. Lee, "Two efficient algorithms for the analyses of a nonlinearly loaded antenna and antenna array in the frequency domain," *IEEE Trans. Electromag Compat*, vol. 45, pp: 339–346, 2000.
- [6] K.C. Lee, "Genetic algorithm based analyses of nonlinearly loaded antenna arrays including mutual coupling," *IEEE Trans. Antennas Propagat*, vol. 51, pp: 776–781, 2003.
- [7] K.C. Lee, "Analyses of Nonlinearly Loaded Antennas and Antenna Arrays Using Particle Swarm Algorithm," *IEEE Conference on Antennas Propagat*, 2004.
- [8] K.C. Lee, "Frequency Domain analyses of Nonlinearly Loaded Antenna Arrays Using Simulated Annealing Algorithm," *Prog. Electromagn Res* 78, pp. 265–283, 2005.
- [9] K.C. Lee, "Mutual coupling mechanisms within arrays of nonlinear antennas," *IEEE Trans. Electromag Compat*, vol. 47, pp: 963–970, 2005.
- [10] K.C. Lee, "Application of neural networks and its extension of derivative to scattering from a nonlinearly loaded antenna," *IEEE Trans. Antennas Propagat*, vol. 55, pp. 1126–1132, 2007.
- [11] K.C. Lee, "Application of neural networks and its extension of derivative to scattering from a nonlinearly loaded antenna," *IEEE Trans. Antennas Propag*, vol. 55, no. 3, pp. 1126–1132, 2007.
- [12] K. Sheshyekani, S. H. Sadeghi, and R. Moini, "A combined MoM-AOM approach for frequency domain analysis of nonlinearly loaded antennas in the presence of a lossy ground," *IEEE Trans. Antennas Propagat*, vol. 56, pp. 1717–1724, 2008.
- [13] S. R. Ostadzadeh, M. Tavarani, and M. Soleimani, "A hybrid model in analyzing nonlinearly loaded dipole antenna and finite antenna array in the frequency domain," *International Journal of RF and Microwave*, vol. 19, pp. 512–518, 2009.
- [14] S. R. Ostadzadeh, "An Efficient hybrid model in analyzing nonlinearly loaded dipole antenna above Lossy Ground in the Frequency Domain," *Applied Computational Electromagnetic Society (ACES) Journal*, vol. 28, no. 9, pp.780–787, 2013.
- [15] D. Poljak et al, "Transient Response of Nonlinearly Loaded Wire Antennas in Two-Media Configuration," nonlinearly loaded antenna and antenna array in the frequency domain," *IEEE Trans. Electromag Compat*, vol. 46, no. 1, pp: 121–125, 2004.
- [16] H. R. Karami, and K. Sheshyekani, "Transient response of nonlinearly loaded antennas above a lossy dielectric half-space: A modified AOM approach," *IEEE Trans. Electromag Compat*, vol. 20, pp.1–9, March 2012.
- [17] R. F. Harrington, *Field Computation by Moment Methods*. Macmillan, New York, 1968.
- [18] D. Liao, "Scattering and Imaging of Nonlinearly Loaded Antenna Structures in Half-Space Environments," *IEEE Trans. Antennas Propagat*, vol. 62, no. 8, pp. 4230–4240, 2014.
- [19] D. Liao, "Generalized Wideband Harmonic Imaging of Nonlinearly Loaded Scatterers," *IEEE Trans. Antennas Propagat*, vol. 63, no. 5, pp. 2079–2087, 2015.